Electronic Supplementary Material (ESI) for Journal of Materials Chemistry C.

Supporting Information

Insights into the relationship between molecular and order-dependent photostability of ITIC derivatives for the production of photochemically stable blends

Y. A. Quiroz Avalos,[a] Q. Eynaud,[a] P. Perkhun,[a] A. Rivaton,[b]

W. Köntges,[c] R. R. Schröder,[c] T. Koganezawa,[d] N. Yoshimoto,[e]

A. Kumar Bharwal,[f] D. Duché,[f] C. M. Ruiz,[f] O. Margeat,[a] C. Aumaître,[g]

R. Demadrille,[g,]* C. Videlot-Ackermann,[a,]* J. Ackermann[a,]*

[a] Aix Marseille Univ., CNRS, CINaM, Marseille, France

[b] Univ. Clermont Auvergne, CNRS, SIGMA Clermont, Institut de Chimie de Clermont-Ferrand, F-63000 Clermont-Ferrand, France

[c] Universität Heidelberg, CAM, Centre for Advanced Materials, Heidelberg, Germany

[d] Industrial Application Division, Japan Synchrotron Radiation Research Institute (JASRI), Sayo, Hyogo 679-5198, Japan.

[e] Department of Physical Science and Materials Engineering, Iwate University, Ueda Morioka 020 8551, Japan.

[f] Aix Marseille Univ.,Univ. de Toulon, UMR CNRS 7334, IM2NP, Marseille, France

[g] Univ. Grenoble Alpes, CEA, CNRS, INP, IRIG, SyMMES, 38000 Grenoble, France

Chemical name of Materials:

ITIC 3,9-bis(2-methylene-(3-(1,1-dicyanomethylene)-indanone))-5,5,11,11-tetrakis(4-hexylphenyl)-dithieno[2,3-d:2',3'-d']-s-indaceno[1,2-b:5,6-b']dithiophene

ITIC-4F 3,9-bis(2-methylene-((3-(1,1-dicyanomethylene)-6,7-difluoro)-indanone))-5,5,11,11-tetrakis(4-hexylphenyl)-dithieno[2,3-d:2',3'-d']-s-indaceno[1,2-b:5,6-b']dithiophene

ITIC-Th 3,9-bis(2-methylene-(3-(1,1-dicyanomethylene)-indanone))-5,5,11,11-tetrakis(5-hexylthienyl)-dithieno[2,3-d:2',3'-d']-s-indaceno[1,2-b:5,6-b']dithiophene

PBDB-T (PCE12) Poly[[4,8-bis[5-(2-ethylhexyl)-2-thienyl]benzo[1,2-*b*:4,5-*b*′]dithiophene-2,6-diyl]-2,5-thiophenediyl[5,7-bis(2-ethylhexyl)-4,8-dioxo-4*H*,8*H*-benzo[1,2-*c*:4,5-*c*′]dithiophene-1,3-diyl]])

PBDB-T-2F (PM6) Poly[[4,8-bis[5-(2-ethylhexyl)-4-fluoro-2-thienyl]benzo[1,2-*b*:4,5-*b*′]dithiophene-2,6-diyl]-2,5-thiophenediyl[5,7-bis(2-ethylhexyl)-4,8-dioxo-4*H*,8*H*-benzo[1,2-*c*:4,5-*c*′]dithiophene-1,3-diyl]-2,5-thiophenediyl]

Table S1. GIWAXS data of single materials (PM6, PCE12 and ITIC) and blend systems (PCE12:ITIC and PM6:ITIC-4F) deposited on ZnO buffer layer at indicated thermal annealing temperature (100°C, 150°C or 200°C). The FWHM values are obtained from Gaussian fitting of the IP (100) peaks.

Sample	Temp. (°C)	Material in blend	q_{xy} (Å^{-1}) (100) peak	Peak area(1)	%(2)	FMHW(3)	d(4) (nm)	CCL(5) (nm)
PM6	100		0.293			0.1223	2.14	0.73
PCE12			0.296			0.1045	2.12	0.86
ITIC			0.343			0.1056	1.83	0.85
PCE12:ITIC	100	PCE12	0.280	319.67	53.62	0.05344	2.24	1.68
		ITIC	0.311	276.42	46.37	0.12595	2.02	0.71
PM6:ITIC-4F	100	PM6	0.293	4289.88	46.83	0.0483	2.14	1.86
		ITIC-4F	0.325	4869.8	53.16	0.1414	1.93	0.63
PM6:ITIC-4F	150	PM6	0.292	6003.77	45.28	0.0433	2.15	2.08
		ITIC-4F	0.324	7254.51	54.71	0.1194	1.93	0.75
PM6:ITIC-4F	200	PM6	0.295	10343.18	59.37	0.0464	2.12	1.94
		ITIC-4F	0.399	7076.44	40.62	0.0378	**1.57**	**2.38**

(1) peak area after deconvolution
(2) contribution to the area of the cumulative fit peak
(3) FMHW = full width at half maximum
(4) d = 2 π/q
(5) CCL for crystal coherence length

Table S2. Performances of PM6:ITIC-4F based organic solar cells (size of 0.27 cm^2) at different annealing temperatures applied to the blend. Post-annealing 100°C indicates an annealing treatment to the full devices during 10 minutes.

Annealing temp. (°C)	V_{oc} (V)	J_{sc} (mA/cm2)	FF (%)	PCE (%)
Post-annealing 100°C	0.88	19.97	63.41	11.09
100°C	0.86	20.19	58.52	10.16
150°C	0.82	20.99	56.11	9.66
200°C	0.68	18.26	53.11	6.60

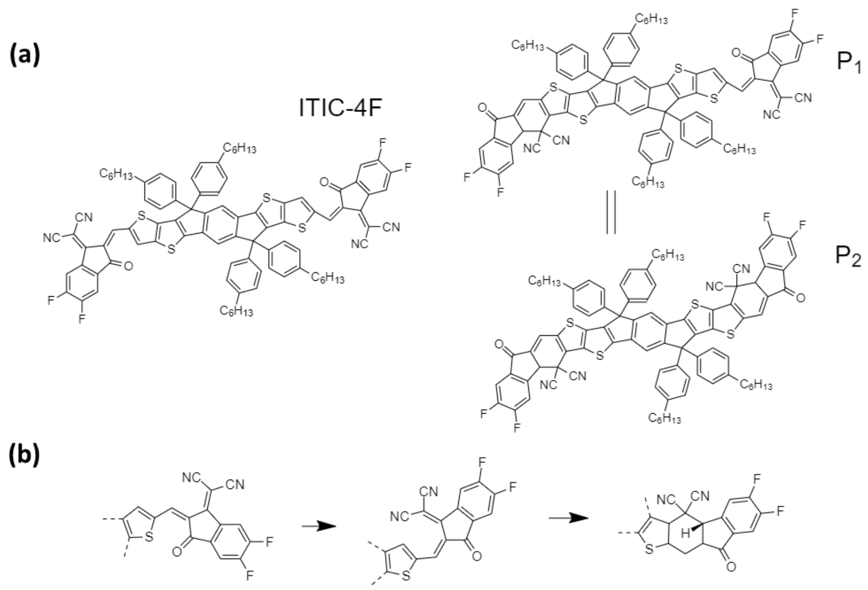

Figure S1. (a) Molecular structure of ITIC-4F and its two isomeric photoproducts P_1 and P_2. (b) Isomerization mechanism of the INCN units. [1]

[1] Y. Che, M. R. Niazi, R. Izquierdo and D. F. Perepichka, *Angewandte Chemie International Edition*, 2021, **60**, 24833–24837.

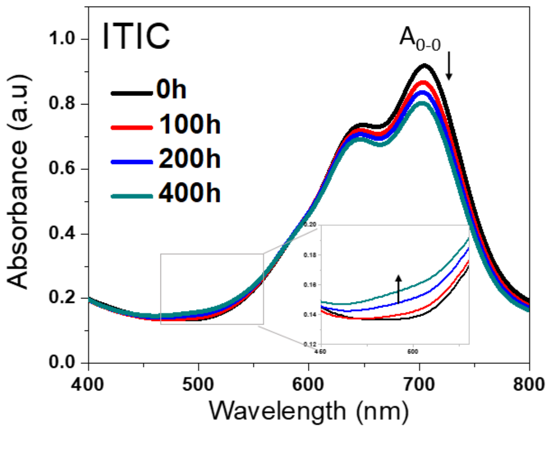

Figure S2. Absorption spectra of ITIC film under constant LED illumination in absence of oxygen.

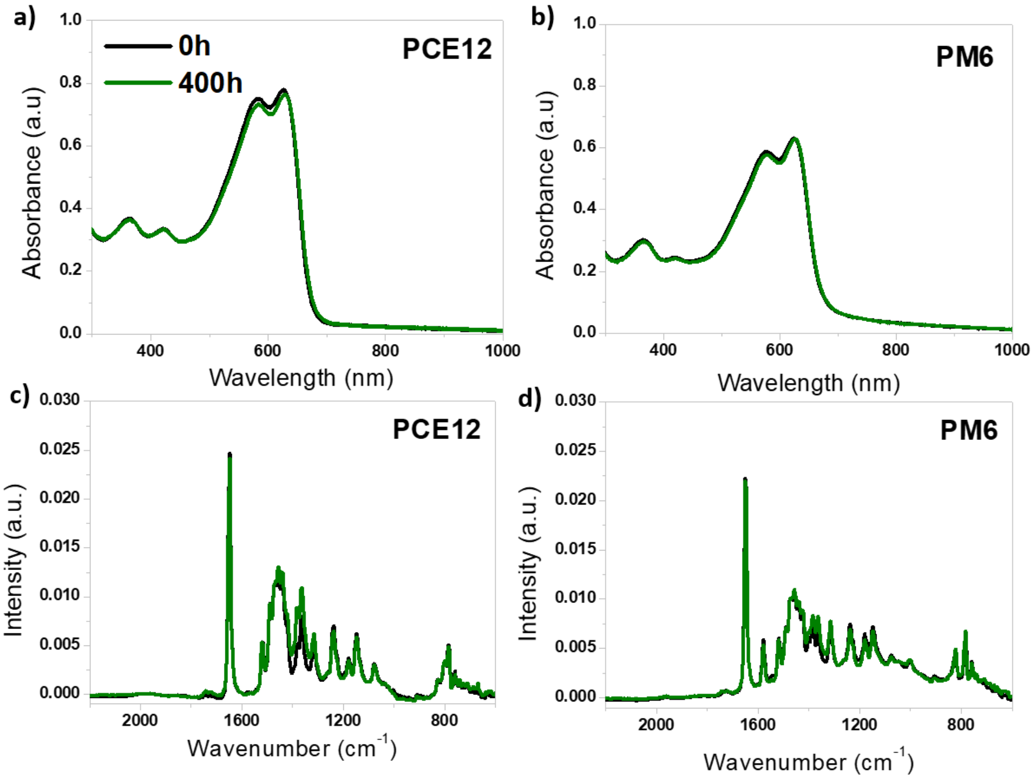

Figure S3. UV-Vis absorption spectra of a) PCE12 and b) PM6, and IR spectra of c) PCE12 and d) PM6 before and after constant 400 h UV-filtered SUNTest illumination in absence of oxygen.

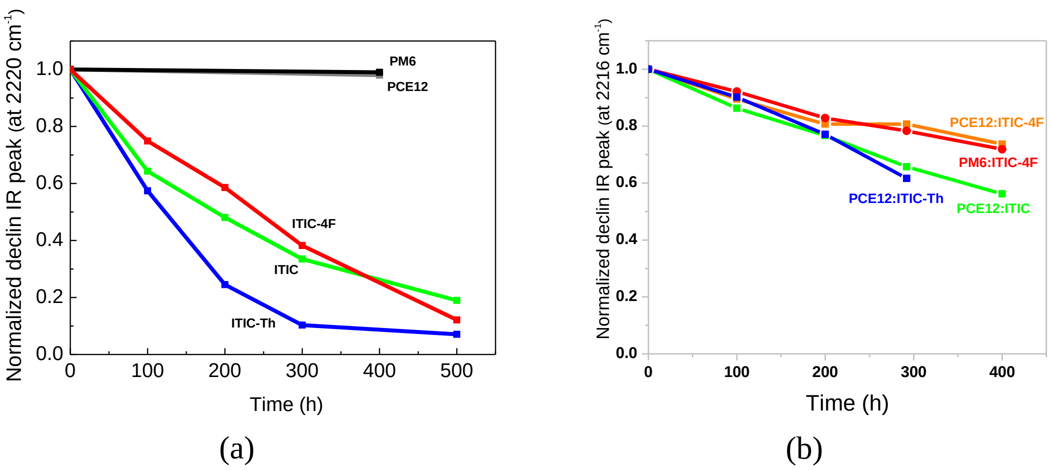

Figure S4. Time evolution of FTIR peaks of NFAs materials (a) and blends (b) under constant UV-filtered SUNTest illumination in absence of oxygen.

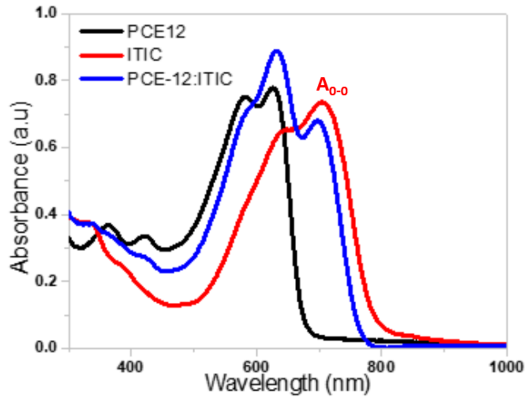

Figure S5. Absorption spectra of PCE12:ITIC blend compared with ITIC and PCE12 materials.

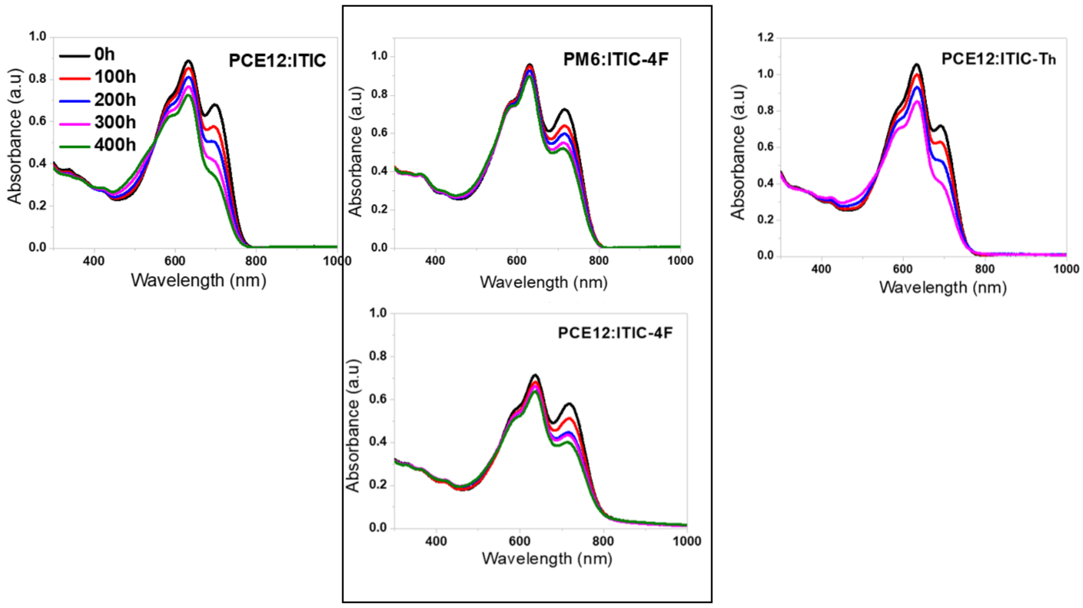

Figure S6. UV-Vis absorption spectra of PCE12:ITIC, PM6:ITIC-4F, PCE12:ITIC-Th and PCE12:ITIC-4F thin films before illumination (0 h in black line) together with the evolution under constant UV-filtered SUNTest illumination in absence of oxygen.

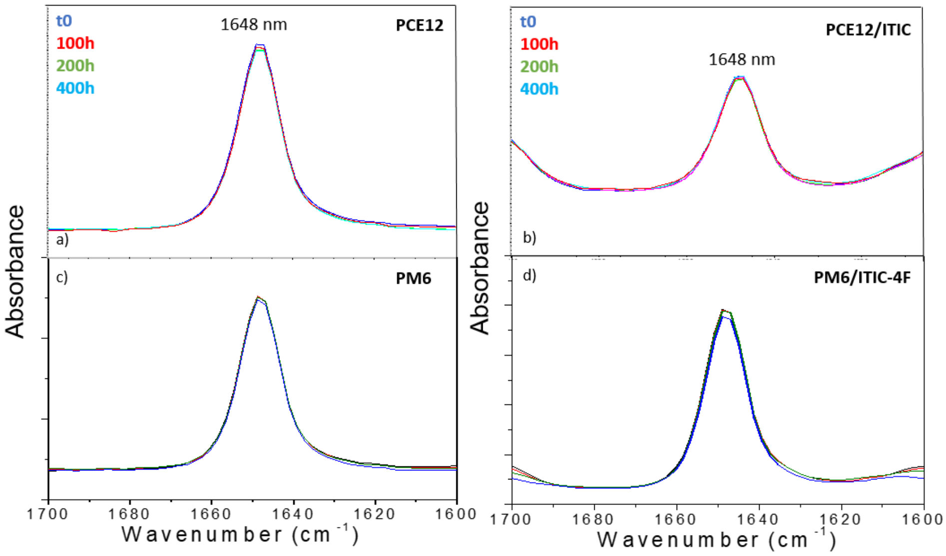

Figure S7. FTIR spectra at 1648 cm^{-1} of a) PCE12 film, b) PCE12:ITIC blend, c) PM6 film and d) PM6:ITIC-4F blend under constant UV-filtered SUNTest illumination in absence of oxygen.

(a)

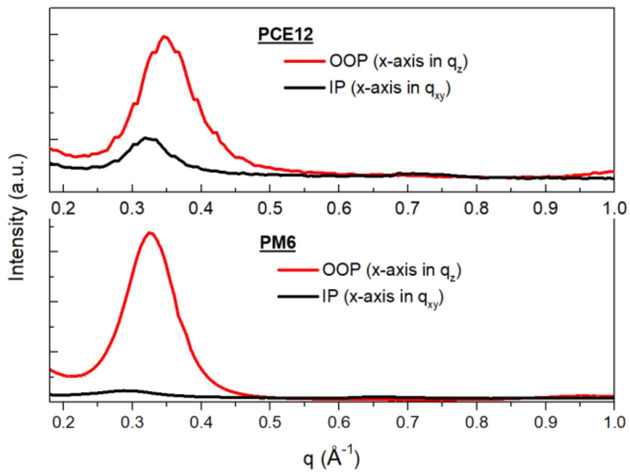

(b)

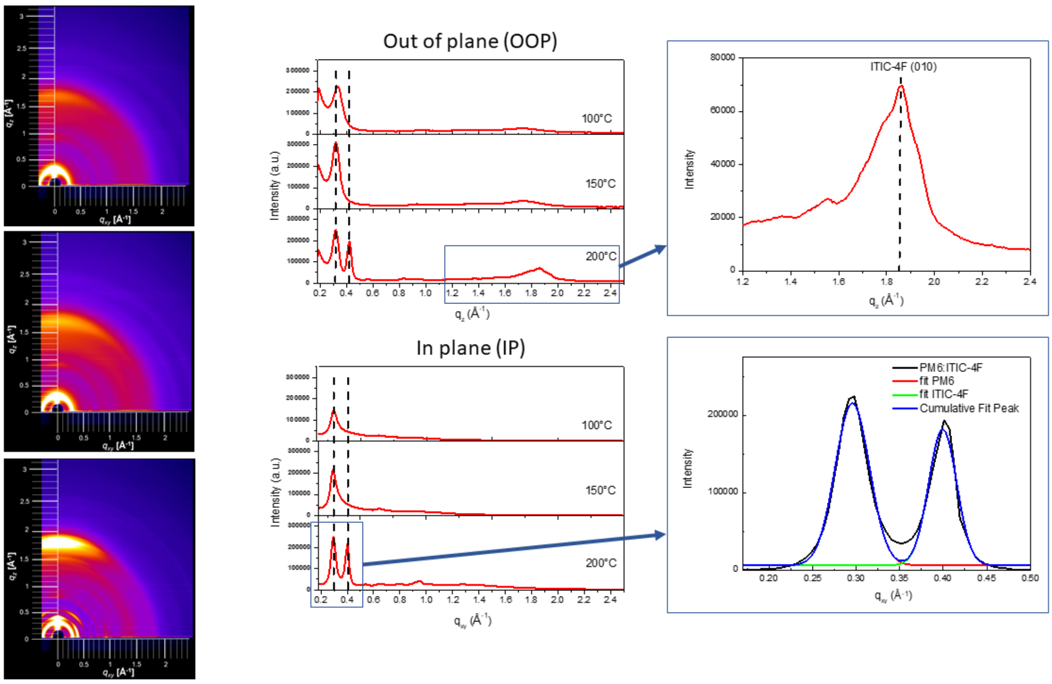

Figure S8. (a) 2D-GIXRD profiles of single PCE12 and PM6 layers at 100°C. (b) 2D-GIXRD patterns and out of plane (OOP) and in plane (IP) profiles of PM6:ITIC-4F blends at 100°C, 150°C and 200°C. Insert: Gaussian fitting of the IP (100) peak of the blend layers.

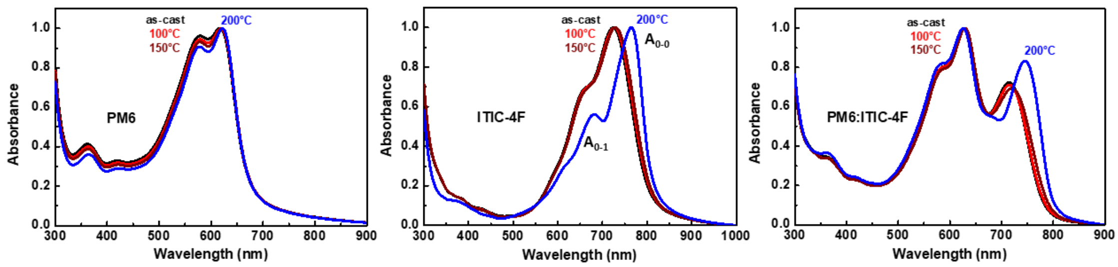

Figure S9. Normalized UV-Vis absorption spectra of single materials and blend films for as-cast and thermal annealed layers at 100°C, 150°C or 200°C.

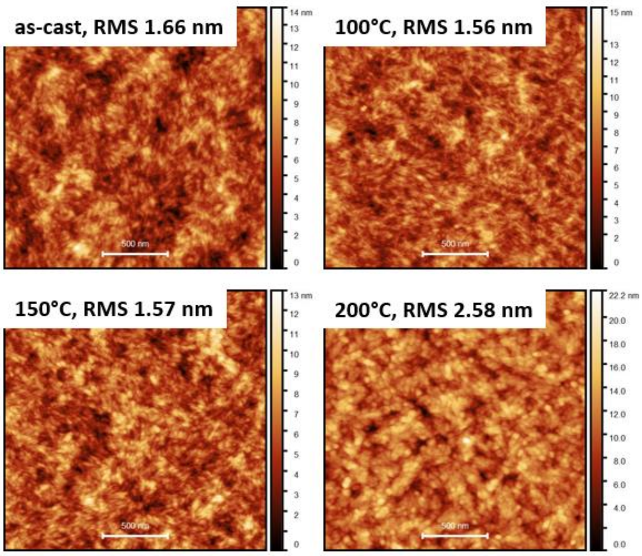

Figure S10. Atomic force microscopy (AFM) phase images showing topographies and root mean square roughness (RMS) of as-cast PM6:ITIC-4F layers and subsequent annealing at 100°C, 150°C and 200°C for 10 min. Scale 2×2 μm.

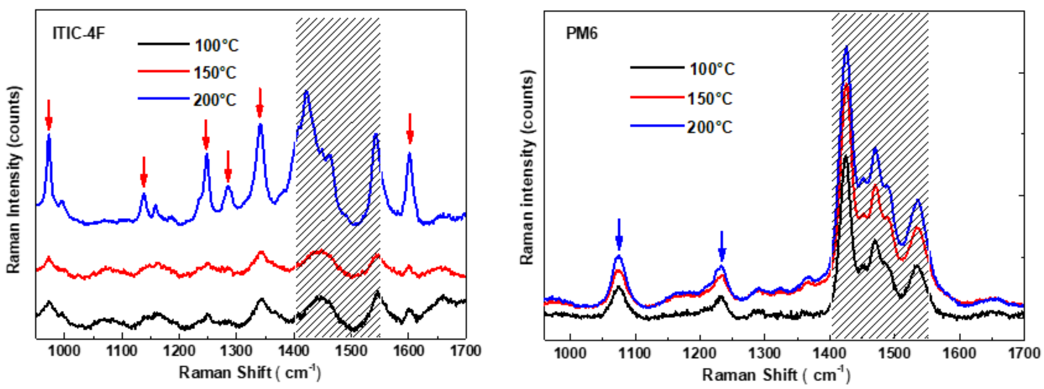

Figure S11. Raman spectra of PM6 and ITIC-4F layers annealed at 100°C, 150°C and 200°C. The layers were annealed after deposition at the indicated temperature for 10 min.

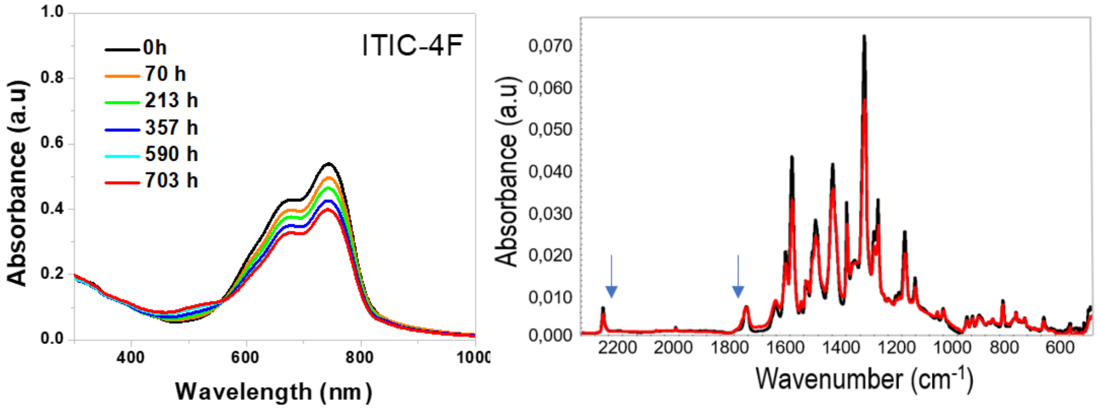

Figure S.12. UV-Vis and IR spectra of ITIC-4F annealed at 200°C under constant UV-filtered SUNTest illumination in absence of oxygen.

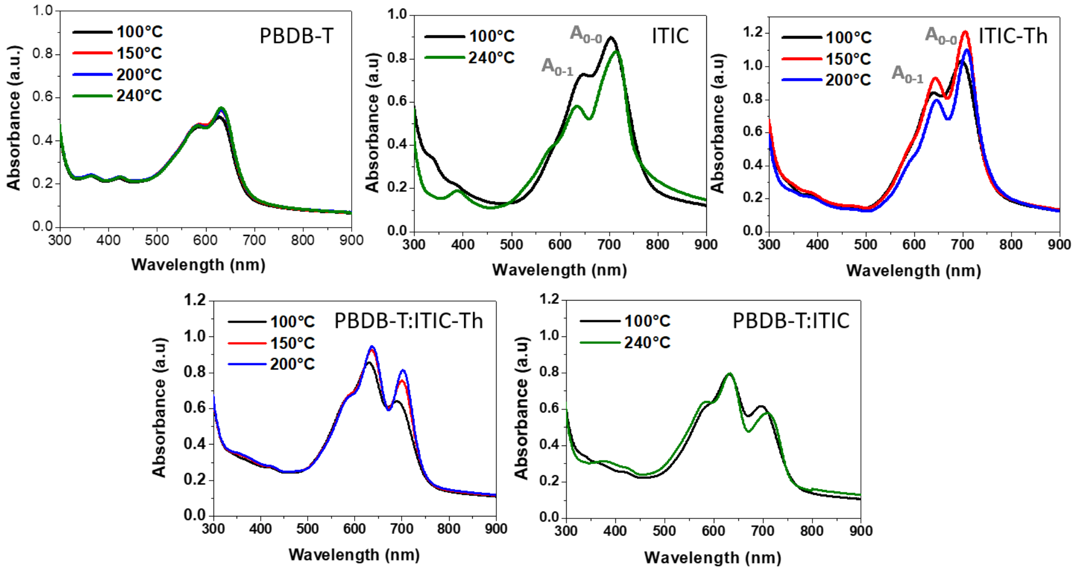

Figure S13. (top) UV-Vis spectra of PBDB-T (PCE12) polymer and NFAs (ITIC and ITIC-Th), (bottom) UV-Vis spectra of PCE12:ITIC and PCE12:ITIC-Th blends at different annealing temperatures. For each blend, layers destined for temperature-dependent studies are produced under the same depositing conditions to guarantee equivalent thicknesses. The layers were post-annealed at the indicated temperature for 10 min.

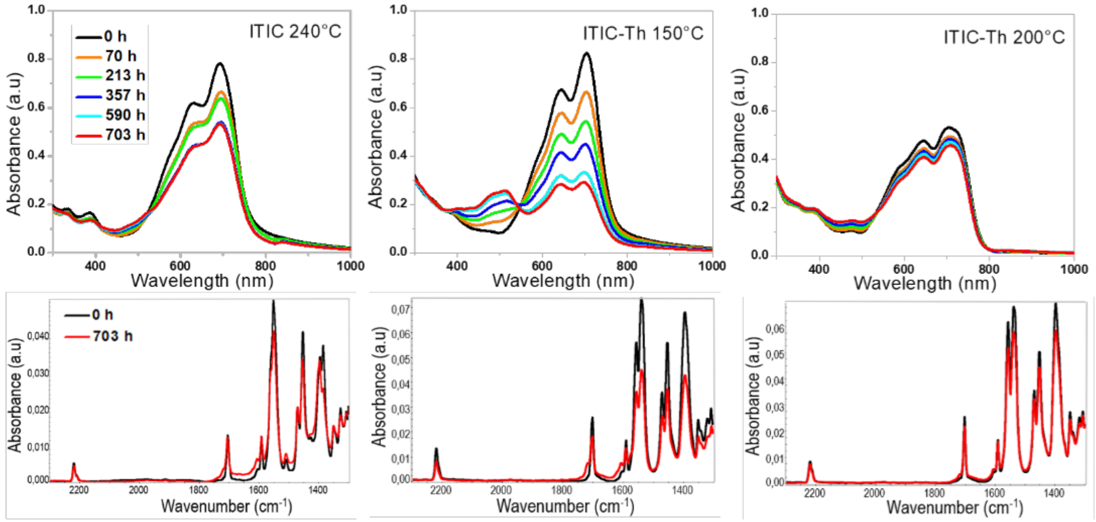

Figure S14. (top) UV-Vis spectra and (bottom) IR spectra of annealed NFA-based films (ITIC and ITIC-Th) under constant UV-filtered SUNTest illumination in absence of oxygen. The layers were annealed after deposition at the indicated temperature for 10 min.

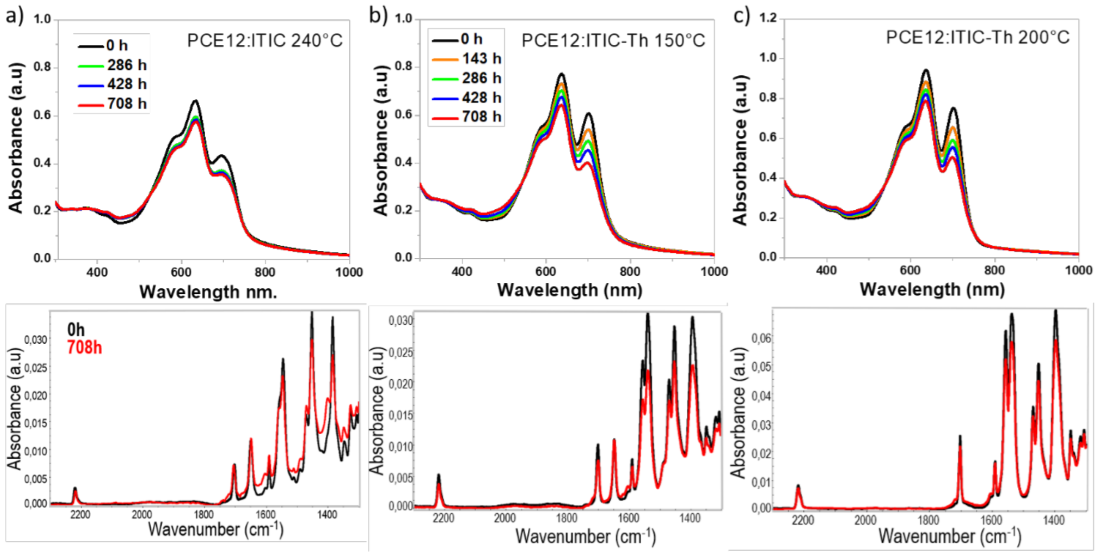

Figure S15. (top) UV-Vis spectra and (bottom) IR spectra of blends: a) PCE12:ITIC at 240°C, b) PCE12:ITIC-Th at 150°C and c) PCE12:ITIC-Th at 200°C under constant UV-filtered SUNTest illumination in absence of oxygen. The layers were annealed after deposition at the indicated temperature for 10 min.

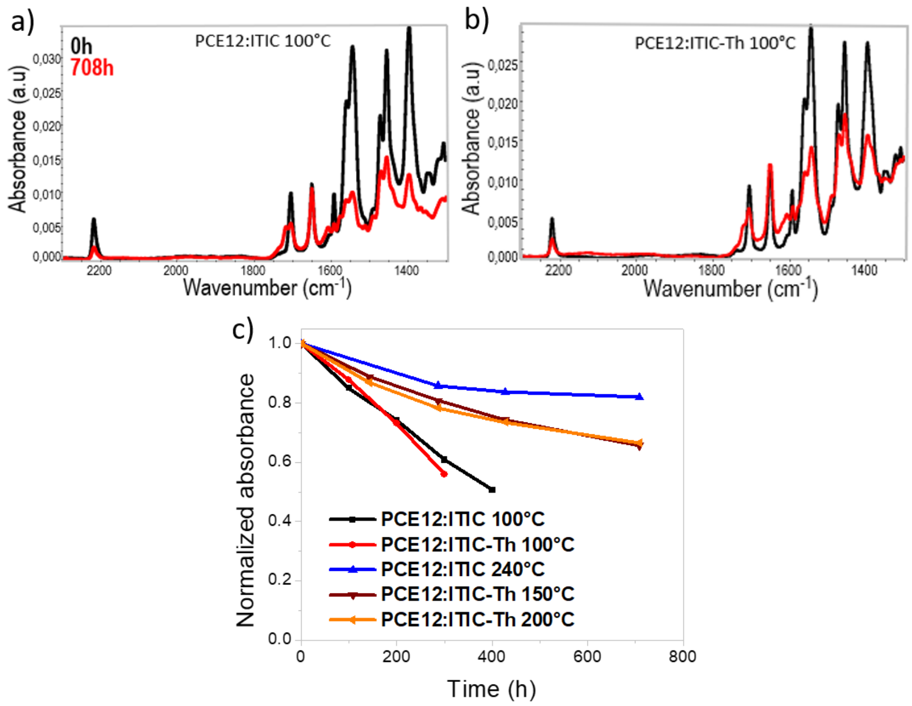

Figure S16. IR spectra of blends a) PCE12:ITIC and b) PCE12:ITIC-Th annealed at 100°C under constant UV-filtered SUNTest illumination in absence of oxygen. c) Normalized degradation kinetics of PCE12:ITIC and PCE12:ITIC-Th at different annealing temperatures calculated from the maximal absorbance of the NFA ($A_{0\text{-}0}$ peak).

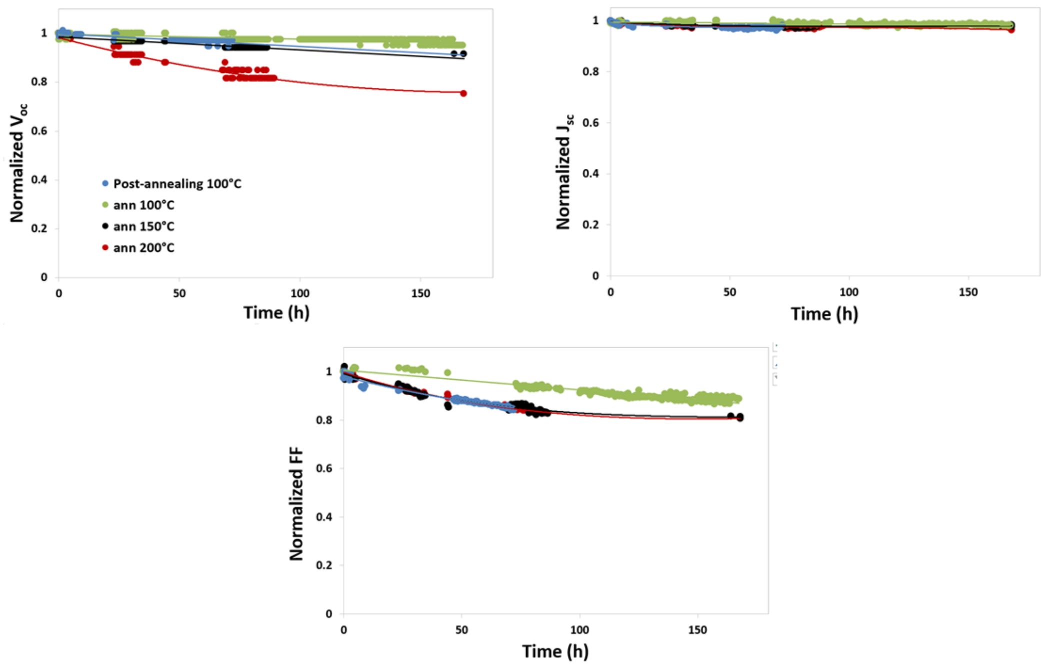

Figure S17. V_{oc}, J_{sc} and FF as a function of illumination time for encapsulated solar cells based on PM6:ITIC-4F blends annealed at different temperatures. Post-annealing 100°C indicates an annealing treatment to the full devices during 10 minutes. Illumination was carried out in a SUNTest where UV light below 400 nm was cut off with an industrial UV filter.